198507: garnet gneissose granulite, Mount Dick

(Youanmi Terrane, Yilgarn Craton)

Blereau, ER, Kelsey, DE and Korhonen, FJ

Location and sampling

Perth (SI 50-14), Northam (2234)

MGA Zone 50, 469671E 6506828N

Warox Site SXWBGD198507

Sampled on 1 June 2010

This sample was collected from a rock pile in a farmer's field along Beering Road, about 4.7 km west of Crows Nest Hill, 2.6 km southeast of Frenches railway station, and 2.3 km northwest of Mount Dick. The sample was collected as part of the Geological Survey of Western Australia's (GSWA) 2003–14 Yilgarn Craton Metamorphic Project, and referred to in that study as sample BG10-4b. The results from this project have not been released by GSWA, although select data have been published in Goscombe et al. (2019).

Geological context

The unit sampled is a gneissose granulite of potentially sedimentary origin within the shear zone system at the western margin of the Youanmi Terrane of the Yilgarn Craton (Quentin de Gromard et al., 2021). The unit is part of a northwest-trending belt of Archean metasedimentary and gneissic rocks referred to by Wilde (2001) and Bosch et al. (1996) as the Jimperding metamorphic belt. The boundary between the South West and Youanmi Terranes in this area is a major, northwest-trending shear zone system (Quentin de Gromard et al., 2021). Four quartzite samples, collected between 13 and 26 km west of this locality, yielded detrital zircon ages between c. 3700 and 3000 Ma, and maximum ages of deposition between c. 3203 and 3005 Ma (GSWA 177901, Wingate et al., 2008a; GSWA 177904, Wingate et al., 2008b; GSWA 177907, Wingate et al., 2008c; GSWA 177908, Wingate et al., 2008d; Pidgeon et al., 2010). Zircon rims in two of these samples have been interpreted to date amphibolite facies metamorphism at c. 2660 Ma (GSWA 177907, Wingate et al., 2008c; GSWA 177908, Wingate et al., 2008d). Zircon geochronology of the sample reported here indicate a potential maximum depositional age for the sedimentary protolith of 2635 ± 2 Ma, with a more conservative age of 2641 ± 8 Ma (Lu et al., 2015). A pelitic migmatite sample collected about 22 km to the south-southeast yielded a weighted mean monazite $^{207}Pb/^{206}Pb$ date of 2664 ± 4 Ma, interpreted as the age of high-grade metamorphism (GSWA 219838, Fielding et al., 2021c). A pelitic granofels sample collected about 86 km to the southeast yielded a weighted mean monazite $^{207}Pb/^{206}Pb$ date of 2647 ± 5 Ma, interpreted as the age of high-grade metamorphism (GSWA 198516, Fielding et al., 2021a). A pelitic gneiss sample collected about 94 km to the southeast yielded a weighted mean monazite $^{207}Pb/^{206}Pb$ date of 2656 ± 6 Ma, interpreted as the age of high-grade metamorphism (GSWA 198522, Fielding et al., 2021b). A summary of the metamorphic evolution of the southwest Yilgarn Craton is provided in Korhonen et al. (2021).

Petrographic description

This sample is a medium- to coarse-grained, weakly foliated gneissose granulite of potentially sedimentary origin consisting of about 51% plagioclase, 23% biotite, 14% garnet, 6% quartz, 4% K-feldspar, 2% apatite and trace amounts of ilmenite, magnetite, zircon (Figs 1, 2; Table 1). Trace orthopyroxene was reported from a feldspathic domain described in the geochronology record for this sample (Lu et al., 2015) but was not observed in the thin section shown in Figure 1. Antiperthitic plagioclase occurs as large grains up to 5 mm in diameter with exsolution of alkali feldspar, and finer (0.2 – 0.6 mm) grains of plagioclase define the matrix together with biotite (Figs 1, 2). Biotite occurs as anhedral laths up to 1.5 mm in size primarily within the matrix, with plagioclase, as well as wrapping around garnet porphyroblasts and large antiperthic plagioclase grains. A distinctly higher concentration of biotite grains with coarser grain size (up to 1.5 mm) occur mantling garnet (Fig. 1). Garnet porphyroblasts are anhedral, up to 6 mm in diameter,

and contain inclusions of biotite, apatite, quartz and rare plagioclase (Figs 1, 2). Quartz is comparatively rare and tends to occur in the matrix proximal to garnet, and is far less common in the plagioclase–biotite-rich matrix of the rock. Quartz grains are up to 3 mm in diameter and feature undulose extinction. K-feldspar occurs as exsolution blebs within plagioclase (Fig. 1), as well as rare discrete, anhedral grains up to 2 mm in diameter in the plagioclase–biotite-rich matrix. Apatite occurs as grains up to 2 mm in diameter in the matrix, as well as included within garnet (Fig. 1). Rare ilmenite and magnetite occur with biotite and quartz in the garnet-bearing portion of the rock. At the hand specimen scale coarse-grained (up to 4–5 mm), pale green plagioclase-rich leucocratic segregations occur as layers and elliptical lenses. These segregations are interpreted to be leucosomes. Millimetre-sized garnet occurs rarely in some of these layers.

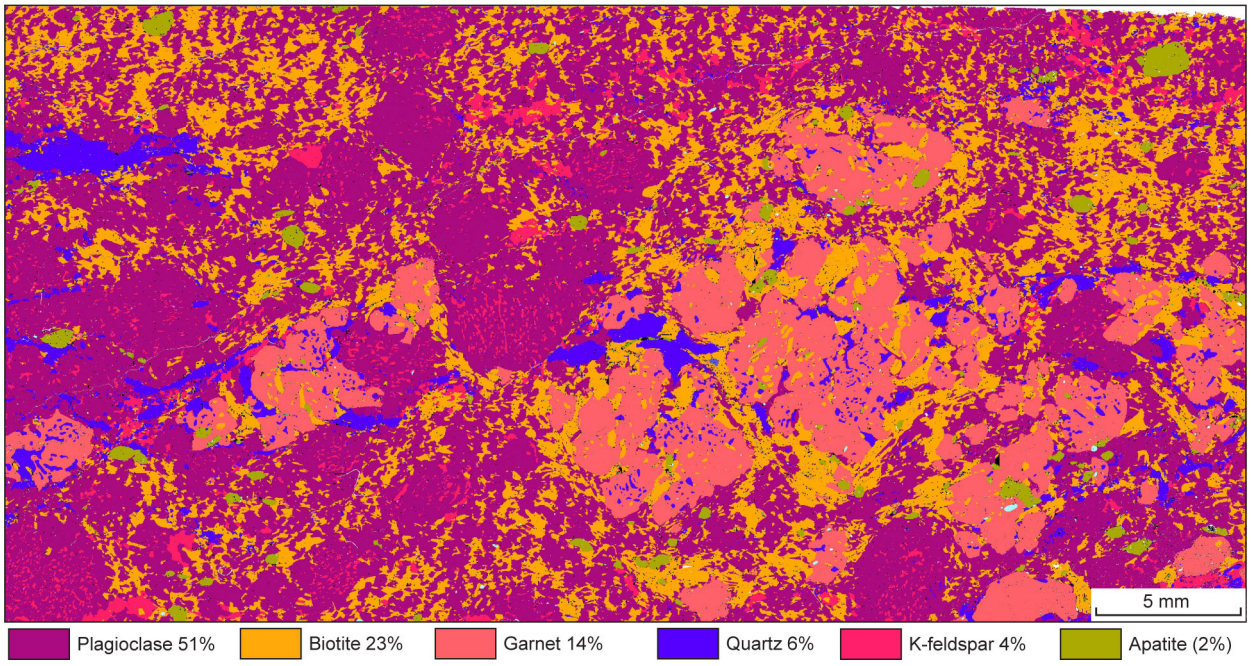

Figure 1. **TESCAN Integrated Mineral Analyser (TIMA) image of an entire thin section from sample 198507: garnet gneissose granulite, Mount Dick. Volume percent proportion of major rock-forming minerals are calculated by the TIMA software**

Table 1. Mineral modes for sample 198507: garnet gneissose granulite, Mount Dick

Mineral modes	*Pl*	*Bt*	*Grt*	*Qz*	*Kfs*	*Ap*	*Mag*	*Ilm*	*Opx*
Observed (vol%)[a]	51	23	14	6	4	2	<0.1	<0.1	unsure
Predicted (mol%)									
@ 820 °C, 5 kbar	60	4	7	14	11	–	0.4	1	1.0
@ 850 °C, 8 kbar	58	2	11	13	13	–	–	1	0.4
@ 810 °C, 8 kbar	60	5	9	14	11	–	–	1	–

NOTES: (a) trace zircon also present in thin section
– not present

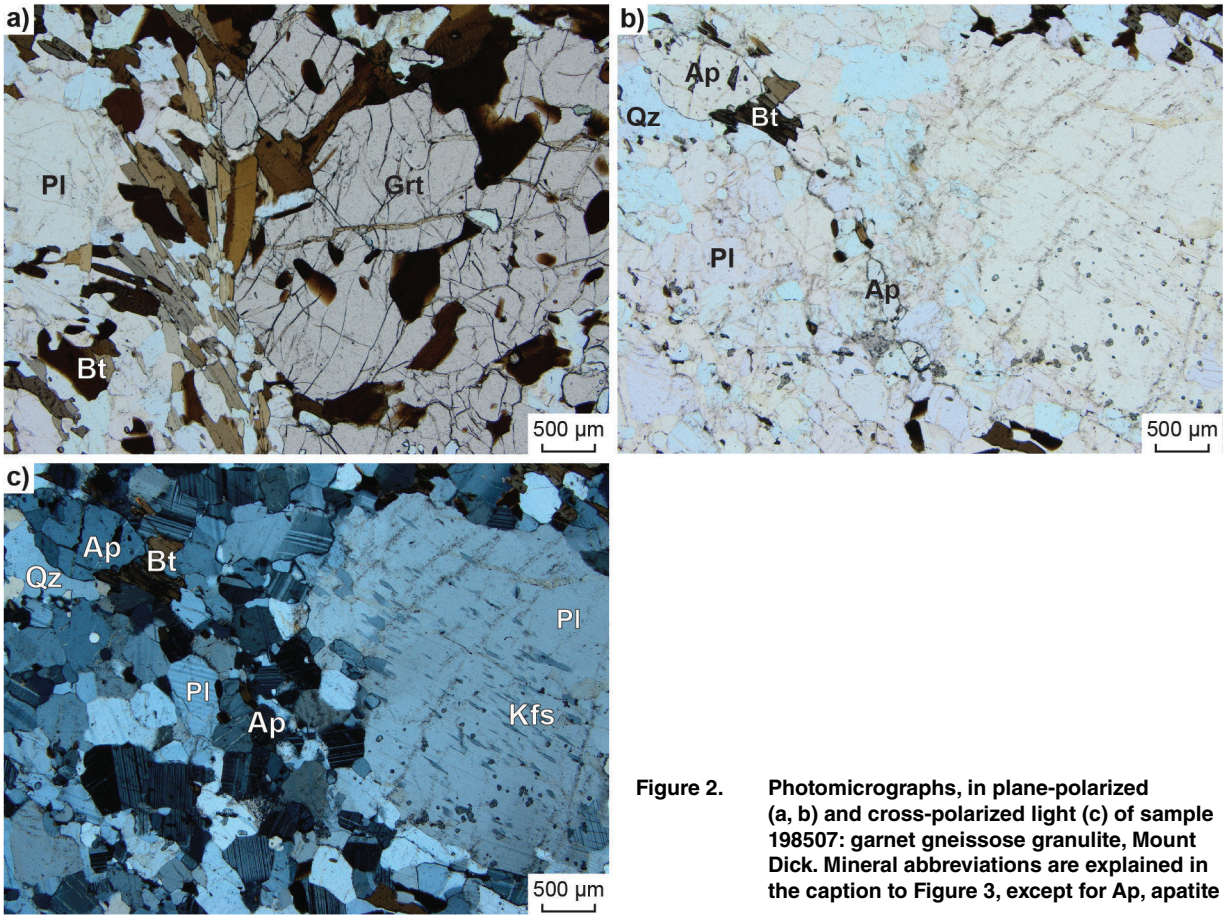

Figure 2. **Photomicrographs, in plane-polarized (a, b) and cross-polarized light (c) of sample 198507: garnet gneissose granulite, Mount Dick. Mineral abbreviations are explained in the caption to Figure 3, except for Ap, apatite**

Analytical details

The metamorphic evolution of this sample was investigated using phase equilibria modelling, based on the bulk-rock composition (Table 2). The bulk-rock composition was determined by X-ray fluorescence spectroscopy, together with loss on ignition (LOI). The modelled O content (for Fe^{3+}) was set at 20% of the measured total Fe. The H_2O content in the modelled bulk composition was reduced from the measured LOI of 0.44 to 0.18 wt% in order to preserve the peak assemblage at conditions below the solidus. The bulk composition was corrected for the presence of apatite by applying a correction to calcium (Table 2). Thermodynamic calculations were performed in the MnNCKFMASHTO ($MnO–Na_2O–CaO–K_2O–FeO–MgO–Al_2O_3–SiO_2–H_2O–TiO_2–O$) system using THERMOCALC version tc340 (updated October 2013; Powell and Holland 1988) and the internally consistent thermodynamic dataset of Holland and Powell (2011; dataset tc-ds62, created in February 2012). The activity–composition relations used in the modelling are detailed in White et al. (2014a,b). Additional information on the workflow with relevant background and methodology are provided in Korhonen et al. (2020).

Results

Metamorphic *P–T* estimates have been derived based on detailed examination of one thin section (Fig. 1), the petrographic description presented in the companion geochronology record (Lu et al., 2015) and the bulk-rock composition. Care was taken to ensure that the thin section and the sample volume selected for whole-rock chemistry were similar in terms of featuring the same minerals in approximately the same abundances, to minimize any potential compositional differences. The *P–T* pseudosection was calculated over a temperature range of 2–10 kbar and 700–900 °C (Fig. 3). The solidus is located between 770–820 °C across the modelled range of pressures. Kyanite is stable above 8.8 kbar at 700 °C. Magnetite is stable at 700 °C at 6.4 kbar and 7.2 kbar at 815 °C. Cordierite is stable across the temperature window, below 3.5 kbar at 700 °C and below 4.7 kbar at 820 °C. Garnet is absent below 3.7 kbar between 710 and 900 °C. Orthopyroxene is stable below 4 kbar at 700 °C and 9.2 kbar at 900 °C (Fig. 3).

Table 2. Measured whole-rock and modelled compositions for sample 198507: garnet gneissose granulite, Mount Dick

XRF whole-rock composition (wt%)[a]												
SiO_2	**TiO_2**	**Al_2O_3**	**Fe_2O_3**	**FeO[b]**	**MnO**	**MgO**	**CaO**	**Na_2O**	**K_2O**	**P_2O_5**	**LOI**	**Total**
60.07	0.65	18.41	–	5.50	0.07	1.33	4.65	4.67	2.40	0.85	0.44	99.04
Normalized composition used for phase equilibria modelling (mol%)												
SiO_2	**TiO_2**	**Al_2O_3**	**O[c]**	**FeO^{T}[d]**	**MnO**	**MgO**	**CaO[e]**	**Na_2O**	**K_2O**	**–**	**H_2O[f]**	**Total**
67.91	0.55	12.27	0.47	4.68	0.07	2.24	4.27	5.12	1.73		0.68	100

NOTES:
(a) Data from Goscombe et al. (2015)
(b) FeO content is total Fe
(c) O content (for Fe_2O_3) set to be 20% of FeO[b]
(d) FeO^T = moles FeO + 2 * moles O
(e) CaO modified to remove apatite: CaO(Mod) = CaO(Total) - (moles CaO(in Ap) = 3.33 * moles P_2O_5)
(f) H_2O content reduced from LOI
– not applicable

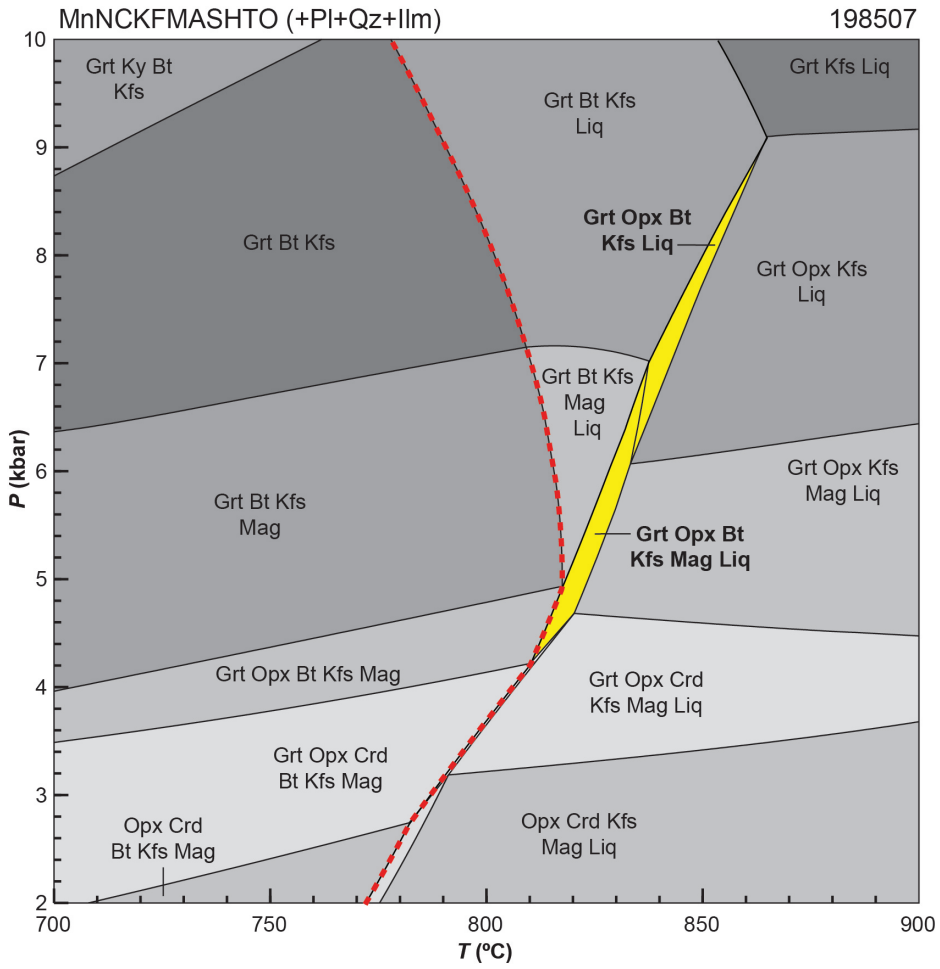

Figure 3. ***P–T*** **pseudosection calculated for sample 198507: gneissose granulite, Mount Dick. Assemblage fields corresponding to peak metamorphic conditions are shown in bold text and yellow shading. Red dashed line represents the solidus. Abbreviations: Bt, biotite; Crd, cordierite; Grt, garnet; Ilm, ilmenite; Kfs, K-feldspar; Ky, kyanite; Liq; silicate melt; Mag, magnetite; Opx, orthopyroxene; Pl, plagioclase; Qz, quartz**

Interpretation

The interpreted peak metamorphic assemblage of garnet–orthopyroxene–plagioclase–quartz–biotite–K-feldspar–ilmenite–melt±magnetite is stable between 810 and 835 °C at 4.2 – 7.0 kbar with magnetite, and between 835 and 865 °C at 6.1 – 9.1 kbar without magnetite, as shown by the yellow-coloured fields in Figure 3. Orthopyroxene is assumed to be part of the peak assemblage but its presence and mode of occurrence cannot be verified. At least some biotite is interpreted to be part of the peak assemblage. The peak assemblage stability fields are bound by cordierite or magnetite stability to lower pressure, loss of biotite stability to higher temperature, and loss of orthopyroxene stability at higher pressure and lower temperatures.

There is limited information on the prograde and retrograde segments of the *P–T* path. The preservation of the observed garnet–orthopyroxene–plagioclase–quartz–biotite–K-feldspar–ilmenite–magnetite assemblage constrains conditions of melt crystallization to be 810–820 °C at 4.2 – 4.9 kbar (Fig. 3), following peak metamorphism. Some coarser grained biotite mantling garnet may be of post-peak, retrograde origin, which may account for some of the discrepancy between the observed mode and the predicted mode within the peak field (Table 1). The growth of retrograde biotite would indicate a cooling-related path, but the amount of pressure change that could have been associated with that is unconstrained. As such, it is not possible to constrain the overall shape of the *P–T* path.

Based on the results from phase equilibria modelling, peak metamorphic conditions are estimated at 810–865 °C and 4.2 – 9.1 kbar, with an apparent thermal gradient between 95 and 190 °C/kbar, and final melt crystallization at 810–820 °C and 4.2 – 4.9 kbar.

References

Bosch, D, Bruguier, O and Pidgeon, RT 1996, Evolution of an Archean metamorphic belt: A conventional and SHRIMP U–Pb study of accessory minerals from the Jimperding metamorphic belt, Yilgarn Craton, Western Australia: The Journal of Geology, v. 104, p. 695–711.

Fielding, IOH, Wingate, MTD Korhonen, FJ and Rankenburg, K 2021a, 198516: pelitic granofels, Quajabin Peak; Geochronology Record 1764: Geological Survey of Western Australia, 5p.

Fielding, IOH, Wingate, MTD, Korhonen, FJ and Rankenburg, K 2021b, 198522: pelitic granofels, Tregenza Road; Geochronology Record 1766: Geological Survey of Western Australia, 5p.

Fielding, IOH, Wingate, MTD, Korhonen, FJ and Rankenburg, K 2021c, 219838: granitic gneiss, Mount Mackie; Geochronology Record 1772: Geological Survey of Western Australia, 5p.

Goscombe, B, Blewett, R, Groenewald, PB, Foster, D, Wade, B, Wyche, S, Wingate, MTD and Kirkland, CL 2015, Metamorphic Evolution of the Yilgarn Craton: Geological Survey of Western Australia (unpublished), 910p.

Goscombe, B, Foster, DA, Blewett, R, Czarnota, K, Wade, B, Groenewald, B and Gray, D 2019, Neoarchaean metamorphic evolution of the Yilgarn Craton: a record of subduction, accretion, extension and lithospheric delamination: Precambrian Research, v. 335, article no. 105441, doi:10.1016/j.precamres.2019.105441.

Holland, TJB and Powell, R 2011, An improved and extended internally consistent thermodynamic dataset for phases of petrological interest, involving a new equation of state for solids: Journal of Metamorphic Geology, v. 29, no. 3, p. 333–383.

Korhonen, FJ, Blereau, ER, Kelsey, DE, Fielding, IOH and Romano, SS 2021, Metamorphic evolution of the southwest Yilgarn, in Accelerated Geoscience Program extended abstracts: Geological Survey of Western Australia, Record 2021/4, p. 108–115.

Korhonen, FJ, Kelsey, DE, Fielding IOH and Romano, SS 2020, The utility of the metamorphic rock record: constraining the pressure–temperature–time conditions of metamorphism: Geological Survey of Western Australia, Record 2020/14, 24p.

Lu, Y, Wingate, MTD, Kirkland, CL, Goscombe, B and Wyche, S 2015, 198507: pelitic gneiss, Mount Dick; Geochronology Record 1282: Geological Survey of Western Australia, 5p.

Powell, R and Holland, TJB 1988, An internally consistent dataset with uncertainties and correlations: 3. Applications to geobarometry, worked examples and a computer program: Journal of Metamorphic Geology, v. 6, no. 2, p. 173–204.

Quentin de Gromard, R, Ivanic, TJ and Zibra, I 2021, Pre-Mesozoic interpreted bedrock geology of the southwest Yilgarn, 2021, *in* Accelerated Geoscience Program extended abstracts: Geological Survey of Western Australia, Record 2021/4, p. 122–144.

White, RW, Powell, R, Holland, TJB, Johnson, TE and Green, ECR 2014a, New mineral activity–composition relations for thermodynamic calculations in metapelitic systems: Journal of Metamorphic Geology, v. 32, no. 3, p. 261–286.

White, RW, Powell, R and Johnson, TE 2014b, The effect of Mn on mineral stability in metapelites revisited: New a–x relations for manganese-bearing minerals: Journal of Metamorphic Geology, v. 32, no. 8, p. 809–828.

Wilde, SA, 2001, Jimperding and Chittering metamorphic belts, southwestern Yilgarn Craton, Western Australia — a field guide: Geological Survey of Western Australia, Record 2001/12, 24p.

Wingate, MTD, Bodorkos, S, and Kirkland, CL 2008a, 177901: quartzite, Kowalyou; Geochronology Record 739: Geological Survey of Western Australia, 5p.

Wingate, MTD, Bodorkos, S, and Kirkland, CL 2008b, 177904: quartzite, Windmill Hill; Geochronology Record 740: Geological Survey of Western Australia, 7p.

Wingate, MTD, Bodorkos, S, and Kirkland, CL 2008c, 177907: quartzite, Noondeening Hill; Geochronology Record 741: Geological Survey of Western Australia, 7p.

Wingate, MTD, Bodorkos, S, and Kirkland, CL 2008d, 177908: quartzite, Noondeening Hill; Geochronology Record 742: Geological Survey of Western Australia, 7p.

Links

Metamorphic history introduction document: Intro_2020.pdf

Recommended reference for this publication

Blereau, ER, Kelsey, DE and Korhonen, FJ 2022, 198507: garnet gneissose granulite, Mount Dick; Metamorphic History Record 11: Geological Survey of Western Australia, 6p.

Data obtained: 17 September 2020

Date released: 14 April 2022

This Metamorphic History Record was last modified on 29 March 2022.

Grid references in this publication refer to the Geocentric Datum of Australia 1994 (GDA94). All locations are quoted to at least the nearest 100 m.

WAROX is GSWA's field observation and sample database. WAROX site IDs have the format 'ABCXXXnnnnnnSS', where ABC = geologist username, XXX = project or map code, nnnnnn = 6 digit site number, and SS = optional alphabetic suffix (maximum 2 characters).

Isotope and element analyses are routinely conducted using the GeoHistory laser ablation ICP-MS and Sensitive High-Resolution Ion Microprobe (SHRIMP) ion microprobe facilities at the John de Laeter Centre (JdLC), Curtin University, with the financial support of the Australian Research Council and AuScope National Collaborative Research Infrastructure Strategy (NCRIS). The TESCAN Integrated Mineral Analyser (TIMA) instrument was funded by a grant from the Australian Research Council (LE140100150) and is operated by the JdLC with the support of the Geological Survey of Western Australia, The University of Western Australia (UWA) and Murdoch University. Mineral analyses are routinely obtained using the electron probe microanalyser (EPMA) facilities at the Centre for Microscopy, Characterisation and Analysis at UWA, and at Adelaide Microscopy, University of Adelaide.

Digital data related to WA Geology Online, including geochronology and digital geology, are available online at the Department's Data and Software Centre and may be viewed in map context at GeoVIEW.WA.

Further details of geoscience products are available from:
Information Centre
Department of Mines, Industry Regulation and Safety
100 Plain Street
EAST PERTH WA 6004
Telephone: +61 8 9222 3459 | Email: publications@dmirs.wa.gov.au
www.dmirs.wa.gov.au/GSWApublications